Journal of Nuclear Medicine, published on January 10, 2020 as doi:10.2967/jnumed.119.234542

Targeted optical imaging of the glucagon-like peptide 1 receptor using exendin-4-IRDye800CW

Marti Boss[1], Desiree Bos[1], Cathelijne Frielink[1], Gerwin Sandker[1], Selen Ekim[1], Camille Marciniak[2], Francois Pattou[2], Go van Dam[3], Sanne van Lith[1], Maarten Brom[1], Martin Gotthardt[1], Mijke Buitinga[1]

[1] Department of Radiology and Nuclear Medicine, Radboud University Medical Center, Nijmegen, The Netherlands

[2] Department of General and Endocrine Surgery, University Hospital 2 Lille, Lille, France

[3] Department of surgery, University Medical Center Groningen, Groningen, The Netherlands

Corresponding author:

Marti Boss (PhD student)

Geert Grooteplein-Zuid 10

6500 HB Nijmegen

The Netherlands

+31243613813

marti.boss@radboudumc.nl

ORCID ID: 0000-0002-5837-1803

Requests for reprints should be directed to the corresponding author

This work is supported by BetaCure (FP7/2014–2018, grant agreement 602812). Martin G declares that he is an inventor and holder of the patent “Invention affecting GLP-1 and exendin” (Philipps-Universität Marburg, June 17, 2009). All other authors declare they have no conflicts of interest.

Word count: 4999

Running title: Optical imaging with exendin-IRDye800CW

ABSTRACT

Rationale

The treatment of choice for insulinomas and focal lesions in congenital hyperinsulinism (CHI) is surgery. However, intra-operative detection can be challenging. This could be overcome with intra-operative fluorescence imaging, which provides real-time lesion detection with a high spatial resolution. Here, a novel method for targeted near-infrared (NIR) fluorescence imaging of glucagon-like peptide 1 receptor (GLP-1R) positive lesions, using the GLP-1 agonist exendin-4, labeled with IRDye800CW, was examined *in vitro* and *in vivo*.

Methods

A competitive binding assay was performed using Chinese hamster lung (CHL) cells transfected with the GLP-1R. Tracer biodistribution was determined in BALB/c nude mice bearing subcutaneous CHL-GLP-1R xenografts. *In vivo* NIR fluorescence imaging of CHL-GLP-1R xenografts was performed. Localization of the tracer in the pancreatic islets of BALB/c nude mice was examined using fluorescence microscopy. Laparoscopic imaging was performed to detect the fluorescent signal of the tracer in the pancreas of mini pigs.

Results

Exendin-4-IRDye800CW binds the GLP-1R with an IC_{50} value of 3.96 nM. The tracer accumulates in CHL-GLP-1R xenografts. Subcutaneous CHL-GLP-1R xenografts were visualized using *in vivo* NIR fluorescence imaging. The tracer accumulates specifically in the pancreatic islets of mice and a clear fluorescent signal was detected in the pancreas of mini pigs.

Conclusion

These date provide the first *in vivo* evidence of the feasibility of targeted fluorescence imaging of GLP-1R positive lesions. Intra-operative lesion delineation using exendin-4-IRDye800CW could benefit open as well as laparoscopic surgical procedures for removal of insulinomas and focal lesions in CHI.

Keywords: Optical imaging, exendin, insulinoma, congenital hyperinsulinism, fluorescence

INTRODUCTION

While pre-operative imaging is essential for tumor detection before surgical cancer treatment, translating this information into the operating room is often challenging. Intra-operative optical imaging can provide real-time detection of tumor lesions and thereby contribute to optimal surgical procedures (*1*).

Insulinomas; insulin-producing neuroendrocrine tumors arising from stem cells or pancreatic beta cells, are the most common cause of endogenous adult hyperinsulinemic hypoglycemia (*2*). Persistent hypoglycemia also occurs in neonates and is in most cases caused by CHI. There are two subforms of this disease: focal CHI, caused by focal adenomatous islet cell hyperplasia, and diffuse CHI, resulting from diffuse involvement of pancreatic beta cells (*3*). Symptoms of insulinomas and CHI, caused by episodic hypoglycemia, are severe and include confusion, diplopia and dizziness and, in cases of prolonged hypoglycemia, even seizure, loss of consciousness or death (*4*).

Insulinomas and focal CHI can be completely cured by surgical removal of the lesion. However, these procedures are complicated by the usually small size of the lesions and their proximity to the pancreatic duct and major vessels (*5*). Precise localization of the lesion is of great importance and starts with sensitive pre-operative detection. For insulinomas, this is performed using various imaging modalities; Contrast enhanced CT and MRI with sensitivities around 70% and 90% respectively (*6*), somatostatin receptor PET, for which sensitivities from 33% to 85% are reported (*7,8*) and the more invasive endoscopic ultrasound, with a sensitivity of 75% for detection of insulinomas (*9*). Currently, there is increasing evidence for the superior performance of the novel imaging method GLP-1R SPECT/CT or PET/CT, using radiolabeled exendin-4, a stable analogue of the hormone GLP-1, which specifically binds the GLP-1R on pancreatic beta cells with high affinity (*10*). With this technique, insulinomas are detected with a sensitivity of up to 97.7% (*7,11,12*). Focal CHI is pre-operatively localized using ^{18}F-DOPA

PET/CT with a sensitivity of 85% (*13*). GLP-1R PET is also being investigated as a potentially more sensitive imaging technique for focal CHI (NCT03768518).

However, even after pre-operative visualization of the lesion, intra-operative detection can be challenging, especially in patients with multiple insulinomas, where very small lesions (< 1 cm) are even more common. Intra-operative ultrasound is routinely used for intraoperative localization of insulinomas. In combination with palpation, success rates ranging from 91% to 100% have been reported (*9,14,15*). However, a laparoscopic procedure, which is preferred when enucleation of the lesion is possible, excludes palpation. Radioguided detection of insulinomas has been proven successful only in a limited number of patients to date (*16*). Another interesting option for intra-operative detection of GLP-1R positive lesions is fluorescence imaging, which has a better spatial resolution and could be used for precise delineation of the lesion and fluorescence-guided surgery (*1,17*).

Currently, there is much attention for the development of tracers for intra-operative fluorescence imaging, mostly using NIR fluorophores, which have the benefit of a high penetration depth (5-10 mm) through tissue (*18*). Coupling of the fluorophore to a tumor-targeting moiety is crucial to ensure specific and efficient delivery of a fluorophore to the lesion of interest.
For targeting of insulinomas and focal CHI, the peptide exendin-4 is an attractive targeting agent for optical imaging.

We have developed exendin-4 coupled to the NIR fluorophore IRDye800CW as a specific tracer for fluorescence imaging of insulinomas and focal CHI. We assessed the potential of targeting GLP-1R positive cells *in vitro* and *in vivo* and the feasibility of performing *in vivo* fluorescence imaging with this compound.

MATERIALS AND METHODS

Reagents

Exendin-4-IRDye800CW was supplied by piCHEM (Graz, Austria). IRDye800CW NHS ester was obtained from LI-COR Biosciences (Lincoln, Nebraska, U.S.A.). The N-epsilon amino group of lysine at position 40 was site specifically modified during solid phase peptide synthesis with a mercapto-propionic acid, releasing an unprotected exendin-4 with a free thiol function after triisopropylsilane cleavage. IRDye800CW was modified with a maleimide and coupling to exendin-4 was performed using a thiol reactive crosslinking approach. The purity was >90%. Stock solutions of exendin-4-IRDye800CW were prepared in phosphate-buffered saline (PBS).

Cell Culture

CHL cells stably transfected with the human GLP-1R (*19*) were cultured (at 37°C and 5% CO_2) in Dulbecco's modified Eagle's medium (DMEM) (Thermo Fisher Scientific, Waltham, MA, USA) with 4.5g/L D-glucose and Glutamax, supplemented with 10% fetal calf serum (FCS) (Life technologies, Carlsbad, CA, USA), 100 IU/mL penicillin G, 10 mg/mL streptomycine, 1 mM sodium pyruvate, 0.1 mM non-essential amino acids and 0.5 mg/ml G418 geneticin.

Competitive Binding Assay

The half-maximal inhibitory concentration (IC_{50}) of exendin-4-IRDye800CW, and unlabeled exendin, as a reference, was determined using CHL-GLP-1R cells in a competitive binding assay as described previously (*10,20*). Cells were grown overnight in six well plates (approximately 10^6 cells/well). Exendin-3-DTPA, labeled with ^{111}In as described earlier (*21*), was used as tracer. The cells were washed twice with PBS and incubated for 4 hours on ice with 50,000 cpm ^{111}In-DTPA-exendin-3 in the presence of increasing concentrations of exendin-4-IRDye800CW or exendin-4 (0.1 – 300 nM). After incubation, cells were washed with PBS, solubilized with 2 mL sodium hydroxide (NaOH), collected and the cell-associated activity was measured in a gamma-counter (Wizard 2480, PerkinElmer, Groningen, The Netherlands).

Binding Assay

Receptor specificity of the binding of the exendin-4-IRDye800CW to CHL-GLP-1R cells was determined in a fluorescent binding assay. CHL-GLP-1R cells were grown overnight in 24 well plates to approximately 95% confluency. Cells were washed twice with binding buffer (DMEM supplemented with 0.5% bovine serum albumin (BSA)) and incubated with 300nM exendin-4-IRDye800CW in triplicate with and without a 50x excess of unlabeled exendin-4 (four hours at 37ºC). After incubation, cells were washed twice with PBS, lysed using 200 µl sodium hydroxide per well, collected and transferred to a black flat-bottom 96-well plate. Fluorescence was measured using a TECAN infinite M200 Pro plate reader (Infinite Pro 200, Tecan Austria GmbH, Groedig, Austria) (excitation: 750 nm, emission 795 nm). Standard curves were created and binding percentages to the cells were calculated using Microsoft Office Excel 2007.

Animal Tumor Model

Female BALB/c nude mice (Janvier, Le Genest Saint Isle, France) (age: 6-8 weeks) were housed in individually ventilated cages (6 mice per cage) under non-sterile conditions with ad libitum access to chlorophyll-free animal chow and water. CHL-GLP-1R cells were injected subcutaneously on the right shoulder ($5*10^6$ cells/mouse) in 200 µL DMEM with 4.5 g/L D-glucose and Glutamax. All animal experiments were approved by the institutional Animal Welfare Committee of the Radboud University Medical Centre and were conducted in accordance to the guidelines of the Revised Dutch Act on Animal Experimentation.

In Vivo Biodistribution

Female BALB/c nude mice bearing subcutaneous CHL-GLP-1R xenografts were injected intravenously with various concentrations of exendin-4-IRDye800CW in 200 µL PBS with 0.5% BSA (N=6 mice per group, 3, 10, 30 and 100 µg exendin-4-IRDye800CW). Control mice (N=4) were injected with PBS with 0.5% BSA only. After 4 hours, the mice were sacrificed by CO_2 asphyxiation and blood and organs of the mice were removed and collected in Roche MagNA Lyser tubes (F Hoffmann- La Roche Ltd., Basel, Switzerland), which were weighed before and after organ collection. The circulation time of 4 hours was chosen based on our previous

experience with radiolabeled exendin tracers (*10*). Radioimmunoprecipitation assay (RIPA) lysis buffer (500 µL; 50mM (hydroxymethyl)aminomethane-hydrochloride (TRIS-HCl), pH 7.4 with 150 mM sodiumchloride (NaCl), 1 mM ethylenediaminetatraacetic acid (EDTA), 1% Triton-X-100 and 1% sodium dodecyl sulphate (SDS)) was added to each tube. Organs were then homogenized using a Roche MagNA Lyser (F Hoffmann-La Roche Ltd., Basel, Switzerland) with repeated cycles of 6000 rpm for 25 seconds with cooling on ice for 1 minute after each cycle. Organ homogenates of control mice were used to create standard curves for each organ. Organ homogenates (100 µl) and the standards were transferred in triplicate to a black flat-bottom 96-well plate. Fluorescence was measured using a TECAN infinite M200 Pro plate reader (Infinite Pro 200, Tecan Austria GmbH, Groedig, Austria) (excitation 750 nm, emission 795 nm). Standard curves were created and tracer uptake in the various organs were calculated using Microsoft Office Excel 2007. Tracer uptake in each organ type was corrected for the weight of the dissected organ. To determine the specificity of the tumor uptake, an additional biodistribution experiment was performed with two groups of mice (n=6 per group), which were injected with 3 µg exendin-4-IRDye800CW with co-injection of 150 µg unlabeled exendin-4 in one of the groups).

We validated the biodistribution of the fluorescent tracer using a dual labeled version of the exendin-tracer DTPA-exendin-4 (piCHEM, Graz, Austria), labeled with both ^{111}In and Cy5.5, as previously described (*21*). With this tracer, we performed biodistribution studies and we compared the tracer uptake in the different organs based on the fluorescent signal with that of the radioactive signal (Supplemental Figure 1).

In Vivo Fluorescence Imaging of GLP-1R Positive Tumors

To show the feasibility of visualizing GLP-1R positive tumors using *in vivo* fluorescence imaging, BALB/c nude mice bearing subcutaneous CHL-GLP-1R xenografts were injected intravenously with 3 µg exendin-4-IRDye800CW (N=3 per group). One group of mice was co-injected with an excess (150 µg) of unlabeled exendin-4. After 4 hours, fluorescence imaging was performed using the IVIS Lumina closed-cabinet fluorescence scanner (Caliper LifeSciences,

Hopkinton, MA) (excitation 745 nm, autofluorescence correction excitation 640 nm, both measured with the ICG filter). After resection of the tumor lesions, mice were imaged again. Subsequently, the mice were dissected to remove the pancreas. Pancreata were fixed overnight in 4% formalin and embedded in paraffin for fluorescence microscopy and immunohistochemistry as described in the following paragraph.

Fluorescence Microscopy and Immunohistochemistry

Sections of 4 µm were cut at 2 levels, 100 µm apart. One section of each level was deparaffinated in xylene for 2 minutes, after which fluorescence imaging was performed using an Odyssey CLx flatbed fluorescence scanner (800 nm channel, recording time 1-5 minutes, focus 1.0 mm) (LI-COR biosciences, Lincoln, NE, USA). Subsequently, these sections were stained for insulin as previously described (22). Consecutive sections were used for fluorescence microscopy. After deparaffination in xylene (2 times five minutes), cell nuclei were stained with Hoechst (33258, Invitrogen, Waltham, MA, USA). Sections were mounted under a glass cover in modified Kaiser's glycerine. Fluorescence imaging was performed using an inverted microscope (DMI6000B, Leica Biosystems, GmbH, Wetzlar, Germany) equipped with a NIR light source ranging up to 900 nm (X-Cite 200DC, Excelas Excelitas Technologies, Waltham, MA, USA), an NIR filter set (microscope two band- pass filters 850–890 m–2p and a long-pass emission filter HQ800795LP; Chroma Technology Corp, Bellows Falls, VT, USA), a monochrome DFC365 FX fluorescence camera (1·4M Pixel CCD, Leica Biosystems GmbH), and LAS-X software (Leica Biosystems GmbH).

Laparoscopic Imaging of Pancreatic Tracer Uptake in Mini Pigs

The possibility of visualizing tracer uptake in the pancreatic beta cells *in vivo* using a laparoscopic laser device was assessed in mini pigs. This was performed in the Department of Experimental Research of the Lille 2 University Facilities, Lille, France. Surgical interventions were approved by the local ethics committee (IACUC). Three healthy adult Göttingen-like mini pigs (*Sus scrofa,* Denis's breeding, Templeuve, France) were anesthetized using 4% isoflurane (Aerrane,

Baxter, France) after receiving premedication (intramuscular injection of ketamine (Ketamine1000, Virbac, Carros, France, 10 mg/kg of body weight) and xylazine (Sédaxylan, CEVA Santé Animale, Libourne, France, 2.5 mg/kg of body weight)). The mini pigs were infused with 1.3 µg/kg exendin-4-IRDye800CW in 20 mL PBS over 30 minutes through an intravenous catheter in the external jugular vein. Four hours after tracer injection, laparoscopic surgery was performed to access the pancreas upon which fluorescence imaging of the pancreatic head and tail was performed using a laser device emitting light at 800 nm and a fluorescence camera (SurgVision BV, The Netherlands).

Statistical Analyses

Statistical calculations were performed using GraphPad Prism (GraphPad Software, La Jolla, CA, USA). IC_{50} values were calculated by fitting the data with non-linear regression using least squares fit with GraphPad Prism.

RESULTS

Exendin-4-IRDye800CW Specifically Binds the GLP-1R with High Affinity

The IC_{50} values of unlabeled exendin-4 and exendin-4-IRDye800CW were 2.5 nM (95% CI; 1.32 - 4.90) and 4.0 nM (95% CI; 2.9 – 5.5) respectively (Figure 1). While the binding affinity of the labeled peptide is significantly lower compared to the unlabeled peptide ($p < 0.01$), the binding affinity is in the same nanomolar range.

Addition of an excess of unlabeled exendin-4 decreased binding of exendin-4-IRDye800CW to CHL-GLP-1R cells from 4.1 ± 0.4% to 0.3 ± 0.2% ($p < 0.01$) (Supplemental Fig 2A).

Exendin-4-IRDye800CW Accumulates in CHL-GLP-1R Tumors

Absolute tumor uptake of exendin-4-IRDye800CW was 9.6 ± 4.2 µg tracer/g organ with an injected dose of 3 µg and increased dose-dependently to 25.5 ± 2.1 µg/g, 43.2 ± 3.6 µg/g and 62.4 ± 31.8 µg/g with injected doses of 10 , 30 and 100 µg, respectively. Highest uptake of

exendin-4-IRDye800CW was observed in the kidneys, due to renal clearance of the tracer (Figure 2).

Co-injection of an excess of unlabeled exendin-4 decreased the tumor uptake of exendin-4-IRDye800CW from 11.6 ± 1.6% ID/g to 1.3 ± 0.4% ID/g ($p < 0.001$) (Supplemental Fig 2B).

In Vivo Fluorescent Tumor Detection is Feasible

Tumors were clearly visualized by fluorescence imaging (Figure 3A and Supplemental Fig 3). After resection of the tumors, no residual fluorescent signal was detected (Figure 3B). Next to the signal in the tumors, a fluorescent signal was observed in the kidneys. In the mice receiving an excess of the unlabeled peptide, no fluorescent signal was seen in the tumor while the signal in the kidneys persists, demonstrating the receptor specificity of the uptake of exendin-4-IRDye800CW (Figure 3C).

Exendin-4-IRDye800CW Accumulates Specifically in Murine Pancreatic Islets of Langerhans

Representative images of the islets of one of the mice are shown in Figure 4. The presence of pancreatic islets is clearly indicated by the positive insulin staining. A clear NIR fluorescent signal is observed at the site of the pancreatic islets. The signal appears to be mostly intracellular, which corresponds with the fast internalization of exendin-4 based tracers. A much lower signal is observed in the exocrine pancreatic tissue. The higher fluorescent signal in the pancreatic islets points to receptor specificity of the uptake of exendin-4-IRDye800CW.

Pancreatic Uptake of Exendin-4-IRDye800CW is Detected by In Vivo Laparoscopic Imaging in Mini Pigs

Laparoscopic NIR fluorescence imaging of the pancreas in healthy mini pigs revealed a clear fluorescent signal in the pancreatic head and tail with which it is possible to discriminate between pancreatic tissue and surrounding tissues (Figure 5).

DISCUSSION

Surgery to remove insulinomas or lesions in focal CHI is challenging and carries substantial risks of morbidity (*4,5*). Precise detection of the lesion is essential for an optimal surgical procedure. Real-time intra-operative detection with a high sensitivity and spatial resolution for precise lesion delineation can be provided by targeted fluorescence imaging. An agent for targeted NIR fluorescence imaging of the GLP-1R was developed and examined *in vitro* and *in vivo* in this study.

Exendin-4-IRDye800CW was shown to have a high affinity for the GLP-1R. Because of the high target affinity of the tracer combined with fast clearance from non-target tissues, a signal with high target-to-background values can be achieved.

Exendin-4-IRDye800CW was shown to accumulate dose-dependently in subcutaneous GLP-1R positive tumors in mice. We demonstrate the reliability of the method used to assess the biodistribution of the fluorescent tracer by showing comparable results of fluorescent and radioactive quantification of the uptake of the dual-labeled tracer ^{111}In-DTPA-exendin-4-Cy5.5 in GLP-1R positive tumors, pancreas and kidneys of mice. We furthermore show that with exendin-4-IRDye800CW, subcutaneous GLP-1R positive tumors could be visualized using NIR fluorescence imaging. Co-injection of an excess of unlabeled exendin-4 completely abolished the fluorescent signal in the tumors, demonstrating the receptor-specificity of the tumor uptake. Furthermore, fluorescence microscopy shows uptake of the tracer specifically in the pancreatic islets of these mice.

The first report on intra-operative imaging of insulinomas involved a non-targeted approach based on the NIR dye methylene blue, which showed higher uptake in insulinomas than normal pancreatic tissue in the proper dilution (*23*). A targeted approach, as described in this study, has the benefit of creating signals with higher contrast between the target and surrounding tissue and therefore more precise delineation of the lesion. Exendin-4 has already been shown to be very effective for targeting of GLP-1R positive tumors in pre-clinical as well as clinical studies using

radiolabeled exendin (*7,10,11*). Reiner *et al.* have previously developed NIR imaging agents, based on exendin-4, for the purpose of in vivo quantification of beta cell mass. These tracers were shown to bind the GLP-1R with high affinities (IC_{50}: 0.3 – 3 nM) and a fluorescent signal was observed in the pancreatic islets. However, uptake of these tracers in GLP-1R positive tumors leading to a possible application for fluorescent-guided surgery was not assessed (*24,25*). Exendin-4 was used by Brand *et al.* to develop a dual-labeled tracer (^{64}Cu-exendin-4-Cy5) for combined PET and fluorescence imaging of GLP-1R positive tumors. While the affinity of this tracer for the GLP-1R (IC_{50}: 50 nM) was lower than exendin-4-IRDye800CW, specific accumulation in GLP-1R tumors was shown and GLP-1R positive xenografts were visualized using *in vivo* PET imaging. However, while a fluorescent signal in the xenografts was detected using fluorescence microscopy, *in vivo* fluorescent imaging was not performed (*26*). We therefore here provide the first evidence of the feasibility of targeted *in vivo* fluorescence imaging of GLP-1R positive lesions.

Using a laparoscopic NIR fluorescence imaging device, a fluorescent signal of exendin-4-IRDye800CW in the pancreas of mini pigs could be detected. Since the exocrine pancreas in pigs is known to have a relatively high GLP-1R density resulting in a low endocrine-exocrine ratio of GLP-1R expression (*27*), the detected signal is most probably not only originating from the pancreatic islets. In mice, where fluorescence microscopy showed specific uptake of the tracer in the pancreatic islets, the endocrine-exocrine ratio of GLP-1R expression is known to be much higher (*27*). However, even if the NIR fluorescent signal detected with the laparoscope originates from both the endocrine and exocrine pancreas of the mini pigs, the feasibility of using this laparoscopic procedure to detect the NIR fluorescent signal clearly demonstrates the potential for clinical translation of this approach. Despite the background fluorescence signal in the pancreas resulting from uptake of the tracer in healthy pancreatic beta cells, visualization and delineation of insulinomas in humans using this approach is most likely possible, since insulinomas have a very high GLP-1R density in almost 100% of cases (higher than healthy pancreatic islets) (*28*) and

visualization with high tumor-to-background ratios has been achieved with radiolabeled exendin (*7*).

Contributing to the potential for clinical translation of this tracer is the use of the NIR fluorophore IRDye800CW. This dye is widely used in the development of targeted fluorescence imaging approaches and several studies already show the first successful clinical applications using this fluorophore. Detection of primary breast cancer lesions as well as peritoneal metastases of colorectal cancer was shown to be feasible using IRDye800CW coupled to the monoclonal antibody (mAb) bevacizumab (*29,30*). Also, IRDye800CW coupled to the mAb cetuximab was successfully used for detection of glioblastomas (*31*). While the first successful clinical results with targeted NIR intra-operative imaging are obtained with mAb based approaches, various peptide-based NIR imaging approaches have been developed and demonstrated to be successful in preclinical settings for a wide range of cancer types. Also, several clinical trials are ongoing (*32*).

CONCLUSION

We here show the feasibility of *in vivo* fluorescence imaging of GLP-1R positive lesions using the novel tracer exendin-4-IRDye800CW. While applicable in open as well as laparoscopic procedures, this approach could be especially beneficial for laparoscopic procedures, in which surgeons currently rely solely on intra-operative ultrasound. In the future, fluorescence imaging using exendin-4-IRDye800CW could benefit surgical removal of insulinomas as well as focal lesions in CHI by providing sensitive and specific real-time intra-operative optical lesion delineation.

DISCLOSURES

Martin G declares that he is an inventor and holder of the patent “Invention affecting GLP-1 and exendin” (Philipps-Universität Marburg, June 17, 2009). All other authors declare they have no conflicts of interest.

ACKNOWLEDGEMENTS

We thank Bianca Lemmers-van de Weem, Kitty Lemmens-Hermans, Iris Lamers-Elemans, Karin de Haas-Cremers and Mike Peters for their technical assistance in the animal experiments.

KEY POINTS

Question

Is targeted fluorescence imaging a feasible technique to improve intraoperative detection of insulinomas and focal lesions in CHI?

Pertinent Findings

Exendin-4-IRDye800CW binds the GLP-1R with an IC_{50} value of 3.96 nM. The tracer accumulates in CHL-GLP-1R xenografts. Subcutaneous CHL-GLP-1R xenografts were visualized using *in vivo* NIR fluorescence imaging and no signal remained after fluorescence-guided resection. The tracer accumulates specifically in the pancreatic islets of mice and a clear fluorescent signal was detected in the pancreas of mini pigs.

Implications for Patient Care

Targeted optical imaging of GLP-1R positive lesions could benefit surgical treatment of insulinomas and CHI by providing sensitive and specific real-time intra-operative optical lesion delineation.

REFERENCES

1. de Boer E, Harlaar NJ, Taruttis A, et al. Optical innovations in surgery. *Br J Surg.* 2015;102:e56-72.

2. Kinova MK. Diagnostics and treatment of insulinoma. *Neoplasma.* 2015;62:692-704.

3. Lord K, Dzata E, Snider KE, Gallagher PR, De Leon DD. Clinical presentation and management of children with diffuse and focal hyperinsulinism: a review of 223 cases. *J Clin Endocrinol Metab.* 2013;98:E1786-1789.

4. Senniappan S, Shanti B, James C, Hussain K. Hyperinsulinaemic hypoglycaemia: genetic mechanisms, diagnosis and management. *J Inherit Metab Dis.* 2012;35:589-601.

5. Richards ML, Gauger PG, Thompson NW, Kloos RG, Giordano TJ. Pitfalls in the surgical treatment of insulinoma. *Surgery.* 2002;132:1040-1049; discussion 1049.

6. Zhu L, Xue H, Sun Z, et al. Prospective comparison of biphasic contrast-enhanced CT, volume perfusion CT, and 3 Tesla MRI with diffusion-weighted imaging for insulinoma detection. *J Magn Reson Imaging.* 2017;46:1648-1655.

7. Antwi K, Fani M, Heye T, et al. Comparison of glucagon-like peptide-1 receptor (GLP-1R) PET/CT, SPECT/CT and 3T MRI for the localisation of occult insulinomas: evaluation of diagnostic accuracy in a prospective crossover imaging study. *Eur J Nucl Med Mol Imaging.* 2018;45:2318-2327.

8. Prasad V, Sainz-Esteban A, Arsenic R, et al. Role of (68)Ga somatostatin receptor PET/CT in the detection of endogenous hyperinsulinaemic focus: an explorative study. *Eur J Nucl Med Mol Imaging.* 2016;43:1593-1600.

9. Mehrabi A, Fischer L, Hafezi M, et al. A systematic review of localization, surgical treatment options, and outcome of insulinoma. *Pancreas.* 2014;43:675-686.

10. Brom M, Joosten L, Oyen WJ, Gotthardt M, Boerman OC. Radiolabelled GLP-1 analogues for in vivo targeting of insulinomas. *Contrast Media Mol Imaging.* 2012;7:160-166.

11. Christ E, Wild D, Ederer S, et al. Glucagon-like peptide-1 receptor imaging for the localisation of insulinomas: a prospective multicentre imaging study. *Lancet Diabetes Endocrinol.* 2013;1:115-122.

12. Luo Y, Pan Q, Yao S, et al. Glucagon-like peptide-1 receptor PET/CT with 68Ga-NOTA-Exendin-4 for Detecting Localized Insulinoma: A Prospective Cohort Study. *J Nucl Med.* 2016;57:715-720.

13. Laje P, States LJ, Zhuang H, et al. Accuracy of PET/CT Scan in the diagnosis of the focal form of congenital hyperinsulinism. *J Pediatr Surg.* 2013;48:388-393.

14. Fendrich V, Bartsch DK, Langer P, Zielke A, Rothmund M. [Diagnosis and surgical treatment of insulinoma--experiences in 40 cases]. *Dtsch Med Wochenschr.* 2004;129:941-946.

15. Kisker O, Bastian D, Frank M, Rothmund M. [Diagnostic localization of insulinoma. Experiences with 25 patients with solitary tumors]. *Med Klin (Munich).* 1996;91:349-354.

16. Christ E, Wild D, Forrer F, et al. Glucagon-like peptide-1 receptor imaging for localization of insulinomas. *J Clin Endocrinol Metab.* 2009;94:4398-4405.

17. DeLong JC, Hoffman RM, Bouvet M. Current status and future perspectives of fluorescence-guided surgery for cancer. *Expert Rev Anticancer Ther.* 2016;16:71-81.

18. Ash C, Dubec M, Donne K, Bashford T. Effect of wavelength and beam width on penetration in light-tissue interaction using computational methods. *Lasers Med Sci.* 2017;32:1909-1918.

19. van Eyll B, Lankat-Buttgereit B, Bode HP, Goke R, Goke B. Signal transduction of the GLP-1-receptor cloned from a human insulinoma. *FEBS Lett.* 1994;348:7-13.

20. Jodal A, Lankat-Buttgereit B, Brom M, Schibli R, Behe M. A comparison of three (67/68)Ga-labelled exendin-4 derivatives for beta-cell imaging on the GLP-1 receptor: the influence of the conjugation site of NODAGA as chelator. *EJNMMI Res.* 2014;4:31.

21. Brom M, Oyen WJ, Joosten L, Gotthardt M, Boerman OC. 68Ga-labelled exendin-3, a new agent for the detection of insulinomas with PET. *Eur J Nucl Med Mol Imaging.* 2010;37:1345-1355.

22. Brom M, Woliner-van der Weg W, Joosten L, et al. Non-invasive quantification of the beta cell mass by SPECT with (1)(1)(1)In-labelled exendin. *Diabetologia.* 2014;57:950-959.

23. Winer JH, Choi HS, Gibbs-Strauss SL, Ashitate Y, Colson YL, Frangioni JV. Intraoperative localization of insulinoma and normal pancreas using invisible near-infrared fluorescent light. *Ann Surg Oncol.* 2010;17:1094-1100.

24. Reiner T, Kohler RH, Liew CW, et al. Near-infrared fluorescent probe for imaging of pancreatic beta cells. *Bioconjug Chem.* 2010;21:1362-1368.

25. Reiner T, Thurber G, Gaglia J, et al. Accurate measurement of pancreatic islet beta-cell mass using a second-generation fluorescent exendin-4 analog. *Proc Natl Acad Sci U S A.* 2011;108:12815-12820.

26. Brand C, Abdel-Atti D, Zhang Y, et al. In vivo imaging of GLP-1R with a targeted bimodal PET/fluorescence imaging agent. *Bioconjug Chem.* 2014;25:1323-1330.

27. Eriksson O, Rosenstrom U, Selvaraju RK, Eriksson B, Velikyan I. Species differences in pancreatic binding of DO3A-VS-Cys(40)-Exendin4. *Acta Diabetol.* 2017;54:1039-1045.

28. Reubi JC, Waser B. Concomitant expression of several peptide receptors in neuroendocrine tumours: molecular basis for in vivo multireceptor tumour targeting. *Eur J Nucl Med Mol Imaging.* 2003;30:781-793.

29. Harlaar NJ, Koller M, de Jongh SJ, et al. Molecular fluorescence-guided surgery of peritoneal carcinomatosis of colorectal origin: a single-centre feasibility study. *Lancet Gastroenterol Hepatol.* 2016;1:283-290.

30. Lamberts LE, Koch M, de Jong JS, et al. Tumor-Specific Uptake of Fluorescent Bevacizumab-IRDye800CW Microdosing in Patients with Primary Breast Cancer: A Phase I Feasibility Study. *Clin Cancer Res.* 2017;23:2730-2741.

31. Miller SE, Tummers WS, Teraphongphom N, et al. First-in-human intraoperative near-infrared fluorescence imaging of glioblastoma using cetuximab-IRDye800. *J Neurooncol.* 2018;139:135-143.

32. Joshi BP, Wang TD. Targeted Optical Imaging Agents in Cancer: Focus on Clinical Applications. *Contrast Media Mol Imaging.* 2018;2018:2015237.

Figures

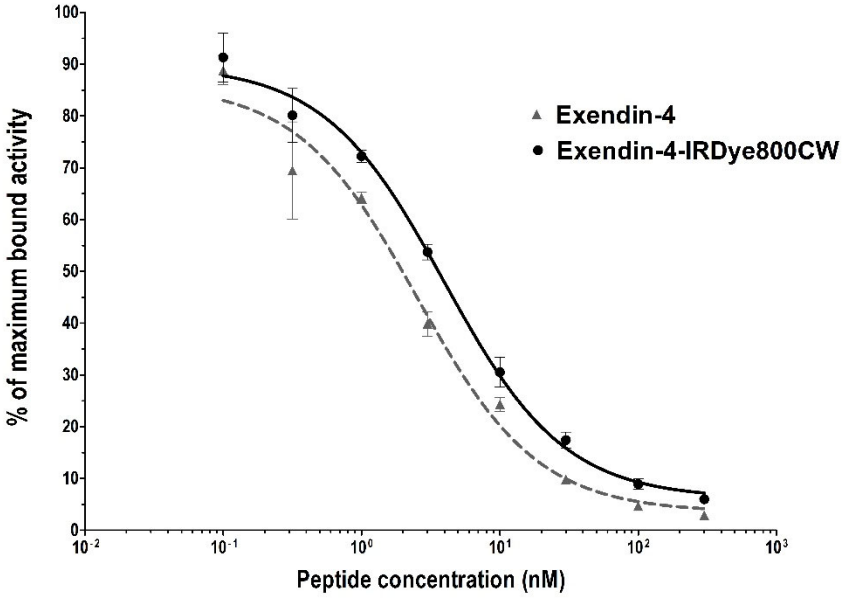

Figure 1. Competition binding assay (IC_{50}) of unlabeled exendin-4 and exendin-4-IRDye800CW on CHL-GLP-1R cells.

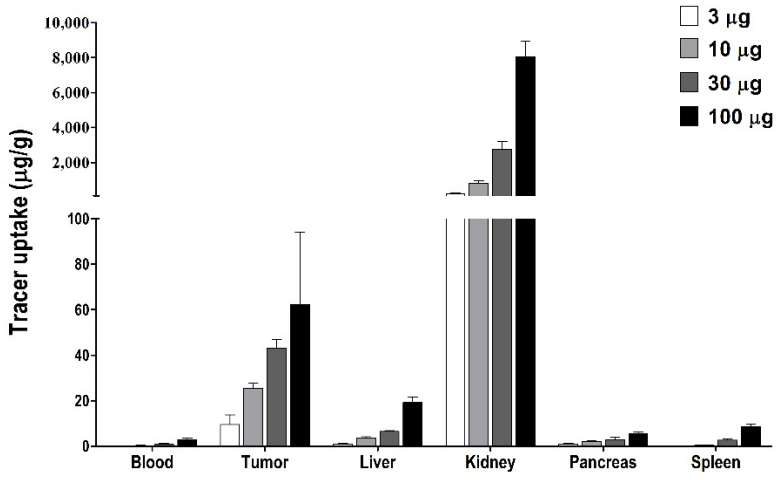

Figure 2. Biodistribution of exendin-IRDye800CW in blood and various tissues of female BALB/c nude mice carrying subcutaneous CHL-GLP-1R tumors (N=6/group) at 4 hours after tracer injection.

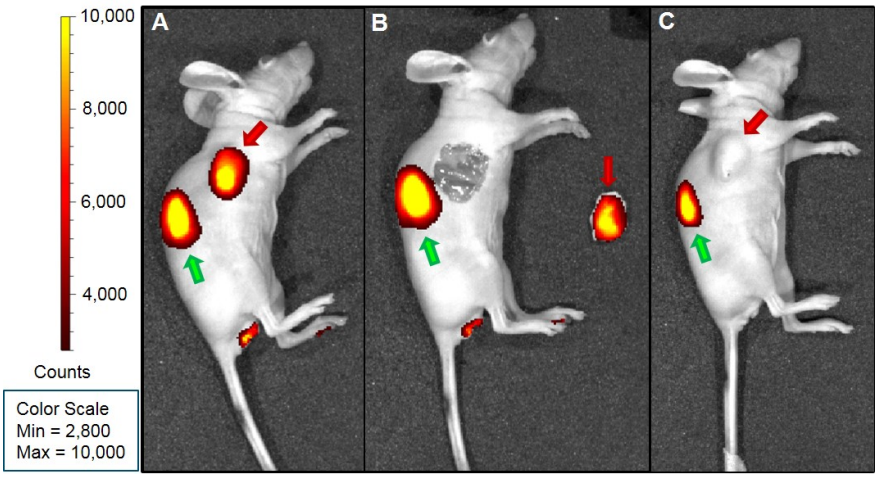

Figure 3. NIR fluorescence images of BALB/c nude mice bearing subcutaneous CHL GLP1-R tumors. Tumors are indicated with red arrows and kidneys with green arrows. (A) Image of an intact mouse. (B) Image of a mouse after resection of the tumor. (C) Image of a mouse injected with the exendin-4-IRDye800CW and an excess of unlabeled peptide.

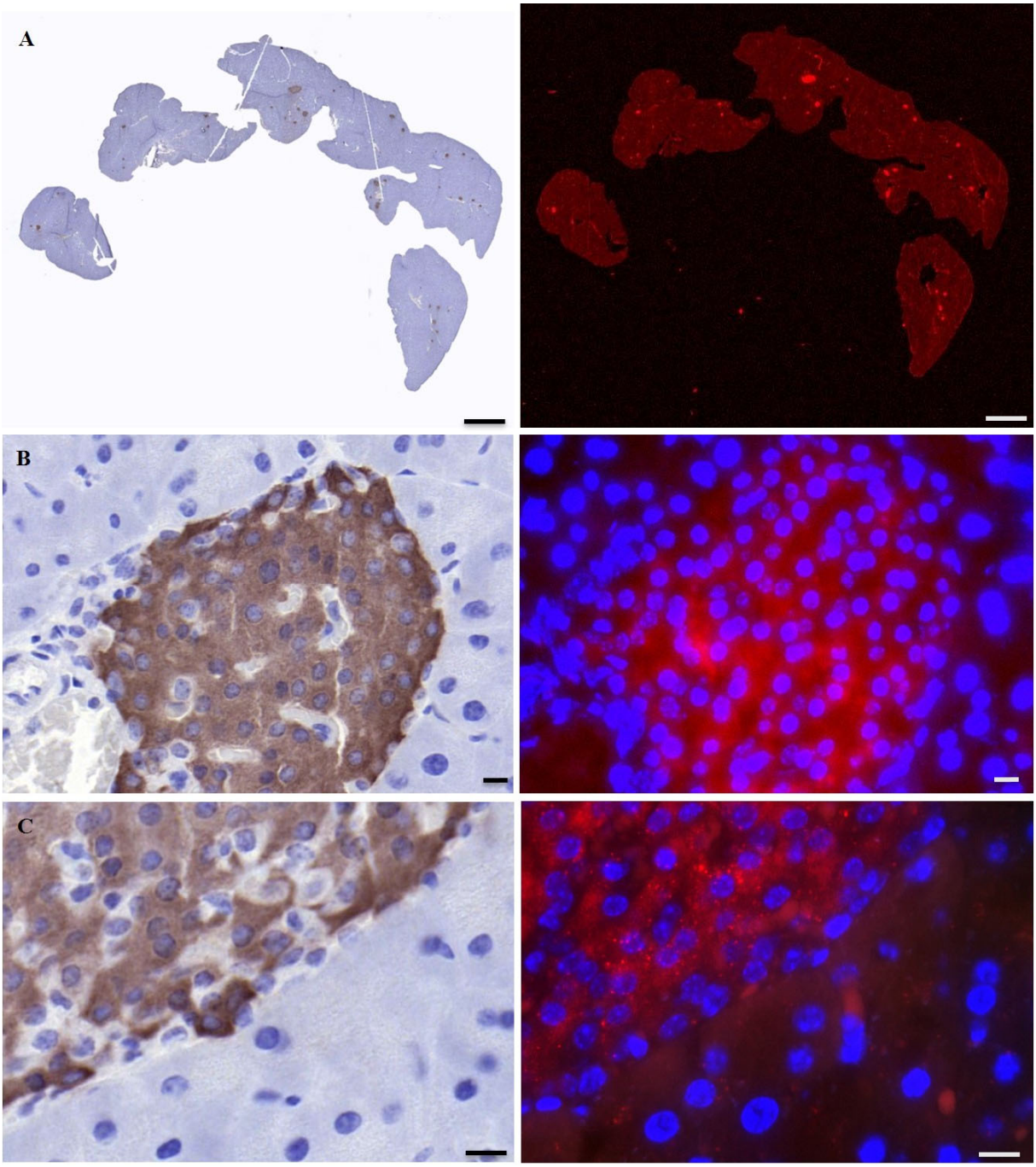

Figure 4: Immunohistochemistry, flat bed fluorescence (A) and fluorescence microscopy (B,C) images of pancreatic tissue of a mouse injected with exendin-4-IRDye800CW. Insulin staining shown in brown (left), 800 nm fluorescent signal in red and nuclei in blue (right). Microscopy images at 40x (B) and 63x (C) magnification. Scale bars indicate 1000 µm (A) or 10 µm (B,C).

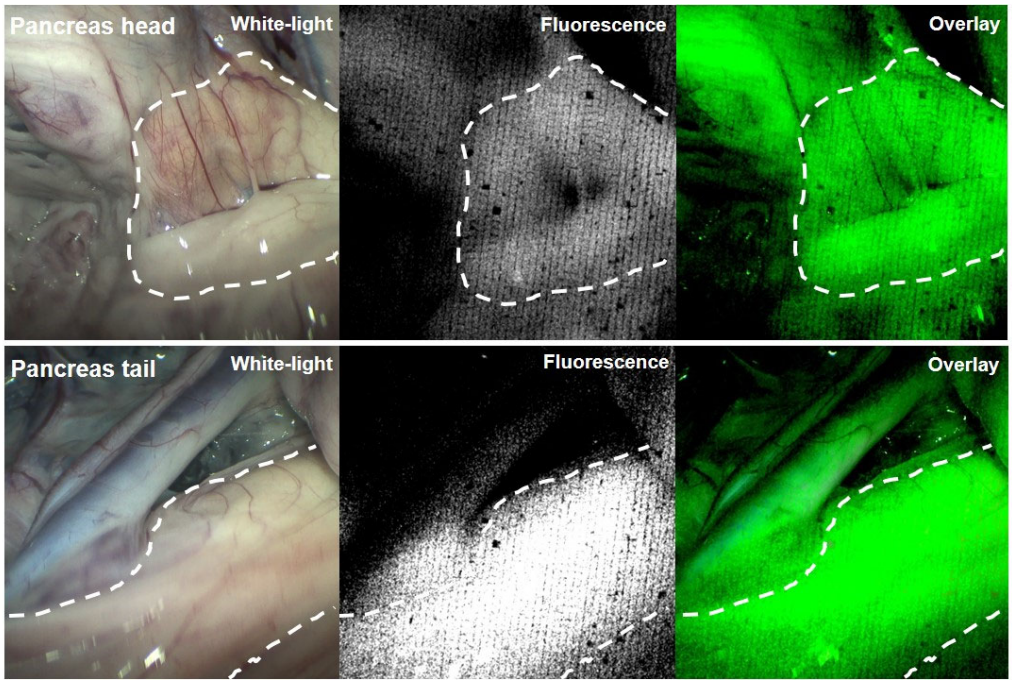

Figure 5. Laparoscopic images of the pancreatic head and tail of a healthy mini pig. On the left white light images, in the middle NIR fluorescent imaging and on the right layover images where the fluorescent signal is depicted in green.

Supplemental figures

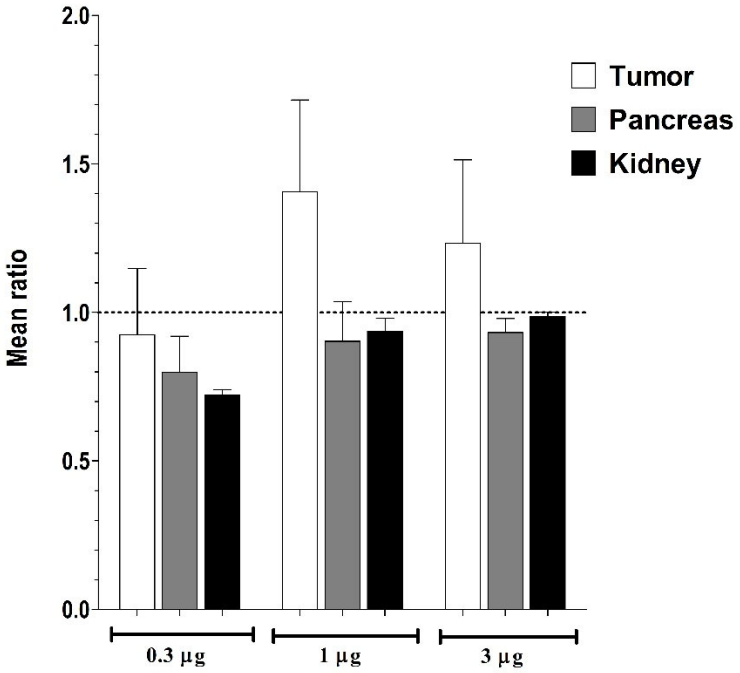

Supplemental Figure 1: Biodistribution of ^{111}In-DTPA-exendin-4-Cy5.5 (0.3 µg, 1 µg and 3 µg, N=6 mice per group) in tumor, pancreas and kidney. Uptake in organs were determined with radiochemical and fluorescent analysis. Given are the ratios of uptake values determined by the different methods showing a good correlation between the methods.

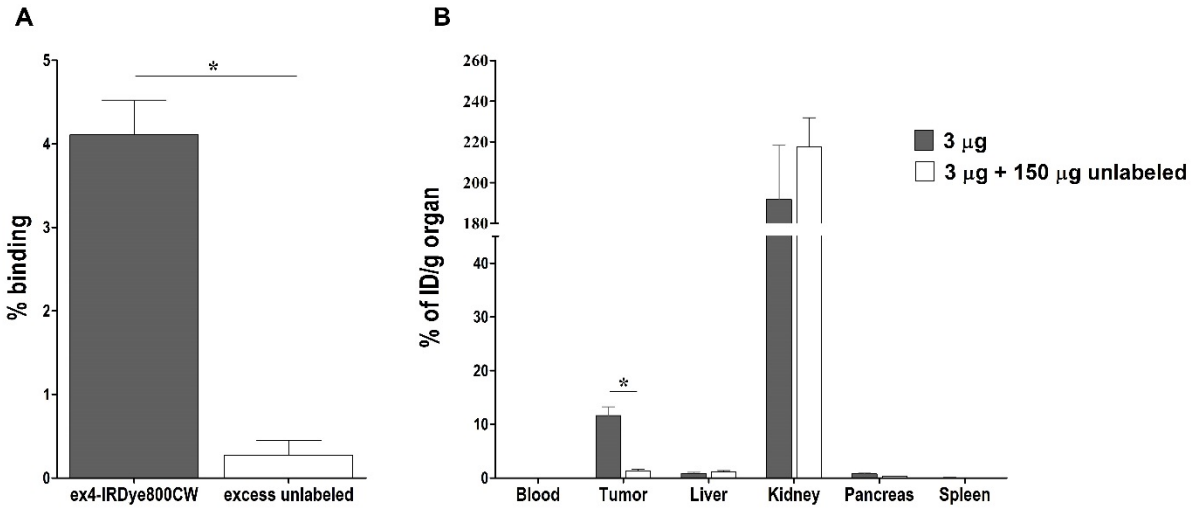

Supplemental Figure 2: Binding of exendin-4-IRDye800CW (300nM) to CHL-GLP-1R cells with and without an excess of unlabeled exendin-4 (N=3) (A). Biodistribution of exendin-IRDye800CW with and without an excess of unlabeled exendin-4 in blood and various tissues of female BALB/c nude mice carrying subcutaneous CHL-GLP-1R tumors (N=6/group) at 4 hours after tracer injection (B).

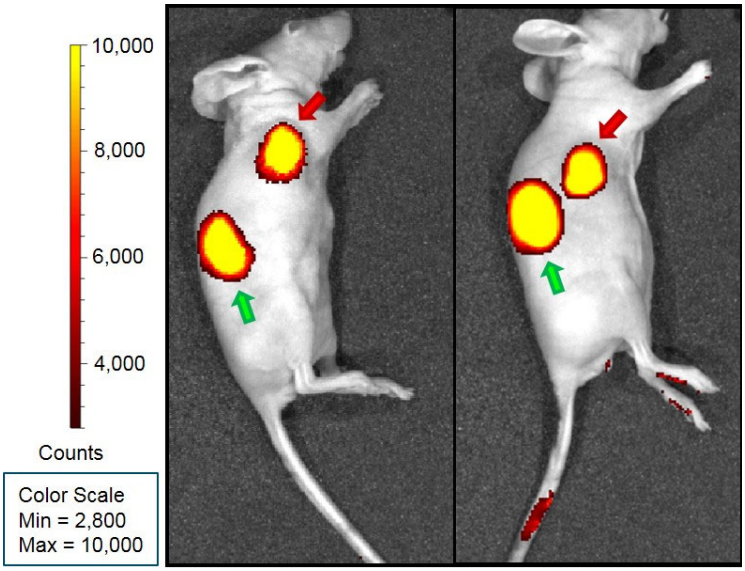

Supplemental Figure 3: NIR fluorescent images of the additional two BALB/c nude mice bearing subcutaneous CHL GLP-1R tumors. Tumors are indicated with red arrows and kidneys with green arrows.